Actuation and Motion Control of Flexible Robots: Small Deformation Problem

Ahmed A. Shabana[1]
Department of Mechanical and Industrial Engineering,
University of Illinois at Chicago,
842 West Taylor Street,
Chicago, IL 60607
e-mail: shabana@uic.edu

Zhengfeng Bai
Department of Mechanical Engineering,
Harbin Institute of Technology,
Weihai 264209, China
e-mail: baizhengfeng@126.com

This paper introduces a new computational approach for the articulated joint/deformation actuation and motion control of robot manipulators with flexible components. Oscillations due to small deformations of relatively stiff robot components which cannot be ignored, are modeled in this study using the finite element (FE) floating frame of reference (FFR) formulation which employs two coupled sets of coordinates: the reference and elastic coordinates. The inverse dynamics, based on the FFR formulation, leads to driving forces associated with the deformation degrees of freedom. Because of the link flexibility, two approaches can be considered to determine the actuation forces required to achieve the desired motion trajectories. These two approaches are the partially constrained inverse dynamics (PCID) and the fully constrained inverse dynamics (FCID). The FCID approach, which will be considered in future investigations and allows for motion and shape control, can be used to achieve the desired motion trajectories and suppress undesirable oscillations. The new small-deformation PCID approach introduced in this study, on the other hand, allows for achieving the desired motion trajectories, determining systematically the actuation forces and moments associated with the robot joint and elastic degrees of freedom, and avoiding deteriorations in the vibration characteristics as measured by the differences between the inverse- and forward-dynamics solutions. A procedure for determining the actuation forces associated with the deformation degrees of freedom is proposed and is exemplified using piezoelectric actuators. The PCID solution is used to define a new set of algebraic equations that can be solved for the piezoelectric actuation voltages required to maintain the forward-dynamics oscillations within their inverse-dynamics limits. A planar two-link flexible-robot manipulator is presented to demonstrate the implementation of the joint/deformation actuation approach. The results obtained show deterioration in the robot precision if the deformation actuation is not considered. [DOI: 10.1115/1.4051438]

Keywords: flexible robots, robot actuation and control, joint/deformation actuation, inverse dynamics, floating frame of reference formulation

1 Introduction

In the *floating frame of reference* (FFR) formulation, widely used in modeling flexible robots, a linear elasticity problem is created and exploited to significantly reduce the number of coordinates and eliminate high-frequency modes of oscillations. These high-frequency modes, in most applications, have a negligible effect on the solution of the problem. Nonetheless, using a modal approach in the FFR formulation leads to challenging problems in the control of robot manipulators that consist of flexible bodies (links). The mode shapes, which describe the body deformation with respect to the FFR body reference, are not associated with discrete physical material points at which actuation forces can be applied. This creates the challenge of defining proper actuation forces and moments that produce the desired motion trajectories. A review of previous investigations has shown that there is no approach available in the literature for defining the actuation forces using the inverse-dynamics constraint forces associated with the finite element (FE)/FFR deformation degrees of freedom. In this paper, this fundamental issue is addressed by developing a new *articulated joint/link deformation actuation approach*, simply referred to as *joint/deformation actuation*. In this approach, the generalized actuation forces associated with the reference and modal coordinates are first determined using an inverse-dynamics procedure. The concept of equipollent systems of forces is used to transform the actuation forces associated with the FFR reference and elastic coordinates to physically meaningful forces of actuation devices such as conventional articulated-joint actuators and motors as well as piezoelectric (PZT) actuators for the deformation control.

The analysis of robot manipulators can be broadly classified into three different groups that require different mathematical approaches. These groups are *rigid-body robots*, *flexible robots*, and *soft robots*. While rigid robots, often modeled using the Newton-Euler equations, are an idealization that implies that the link deformations do not have a significant effect on the robot precision and/or functional operation; flexible-robot dynamics is concerned with the small-deformation problem resulting from the relatively high stiffness of the robot links. For this class of flexible-robot systems, widely used in *manufacturing applications*, the small link deformation can have a significant effect on the robot precision and performance, and therefore, such a small deformation cannot be ignored. The approach most widely used for the analysis of articulated flexible robots is the FFR formulation that allows filtering out insignificant high-frequency modes of vibration while preserving the accuracy of the dynamic model. Soft robots, on the other hand, require using a full finite element (FE) discretization in order to capture the complex deformation shapes.

Precision is an important issue in the design of flexible-robot manipulators, which have several advantages that include lighter weight, smaller actuation-power requirements, higher degree of maneuverability, and less material cost. Several theoretical and experimental investigations have been focused on the dynamics and control of flexible-robot systems [1–9]. For such systems, motion control is a challenging problem in many applications,

[1]Corresponding author.

Contributed by the Mechanisms and Robotics Committee of ASME for publication in the Journal of Mechanisms and Robotics. Manuscript received December 8, 2020; final manuscript received May 28, 2021; published online July 5, 2021. Assoc. Editor: Jozsef Kovecses.

including aerospace, manufacturing, and mechanical engineering [7–17]. In order to improve the motion stability, increase the tracking accuracy, and suppress the vibration of the flexible robotic system; a large number of investigations have been concerned with developing control strategies [18–24]. Certain control strategies have been proposed including sliding mode control [25,26], fuzzy control [27–29], adaptive control [11,30], and neural network control [31,32]. These control strategies are used to design the actuation systems with the goal of achieving the desired accuracy and performance.

The actuation forces of robotic systems are often determined using an inverse-dynamics solution procedure based on *multibody system* (MBS) computational approaches [33–42]. After computing the actuation control forces or torques using control strategies or inverse dynamics, the proper actuators are selected to achieve the desired performance. In the case of flexible robots, two classes of actuators can be recognized; the first includes conventional joint actuators and motors, while the second includes *deformation*- and *shape-control actuators* such as piezoelectric (PZT), shape memory alloy (SMA), and ultrasonic and thermal actuators. Piezoelectric actuators have the advantages of low cost, simple structure, small size, fast response, large force generation, and high control precision [43–45]. Therefore, PZT actuators are widely used in vibration control and trajectory tracking of various flexible-robot manipulators [46–55]. Piezoelectric materials can also be used for both vibration measurement and control of flexible manipulators [56–59].

This paper is focused on using the FE/FFR formulation in which the concept of the reference conditions is fundamental. Different choices of the body coordinate system, defined using different sets of *reference conditions*, lead to different modes and different deformations defined with respect to the selected body coordinate system. The FFR forces associated with these modes may lack any physical interpretation because of the non-unique definition of the deformation modes associated with different body coordinate systems. Consequently, there is a need for a new approach that allows transformation of the forces associated with the FFR modes to actuation forces that have clear physical interpretation and can be used in a hybrid actuation approach for the control of both articulated-joint and deformation degrees of freedom. The concept of the FFR equipollence systems of forces is central for developing such a hybrid control strategy.

2 Scope, Contributions, and Organization of This Investigation

A literature review reveals that the FFR specified-trajectory forces associated with the FE/FFR deformation degrees of freedom have not been considered in the definition of the robot actuation forces. One of the main objectives of this study is to use the FFR force definitions to define physically meaningful actuation forces associated with physical material points or axes of rotations. To this end, a new computational *joint/deformation actuation* approach is developed for the *motion control* of robot manipulators with flexible components whose oscillations cannot be ignored and can negatively impact the robot's precision and functional operations. The small deformations of the stiff robot components are analyzed using the FE/FFR formulation which employs two coupled sets of coordinates; the reference and elastic coordinates. The FFR formulation allows creating a local linear problem that can be exploited to reduce the model dimension by eliminating insignificant high-frequency deformation modes. Because the FFR inverse-dynamics problem leads to driving actuation forces associated with the deformation degrees of freedom, such forces cannot be neglected in the robot control systems. Two different inverse-dynamics problems can be used to determine the actuation forces required to achieve the desired motion trajectories. These are the *partially constrained inverse dynamics* (PCID) and the *fully constrained inverse dynamics* (FCID). The FCID approach, which will be considered in future investigations and allows for *motion and shape control*, can be used to achieve the desired motion trajectories and suppress undesirable oscillations. The new PCID approach introduced in this study, on the other hand, allows achieving the desired motion trajectories, determining the actuation forces and moments associated with the robot joint and elastic degrees of freedom, and avoiding deteriorations in the vibration characteristics as measured by the differences between the inverse- and forward-dynamics solutions. The new procedure for determining the actuation forces associated with the elastic coordinates is exemplified using *piezoelectric actuators*. The PCID solution is used to determine the voltage of the piezoelectric actuation required to maintain the forward-dynamics oscillations within their inverse-dynamics limits. A planar two-link flexible-robot manipulator is presented to demonstrate using the joint/deformation actuation approach proposed in this study. The specific contributions and organization of this paper can be summarized as follows:

(1) A review of the basic FFR kinematic and force equations used in this study is presented in Sec. 3. As discussed in Sec. 3, a force vector that acts at an arbitrary point on a flexible body is equipollent to a system of FFR generalized forces that include forces associated with the deformation coordinates. The FFR forces may lack a clear physical interpretation because of using the *floating coordinate system*.
(2) Using concepts discussed in Sec. 3, *actuation forces* that have clear physical interpretations are developed in Sec. 4. This is accomplished using a point mesh which has a number of points consistent with the number of degrees of freedom of the model. A transformation between the FFR coordinates and the point-mesh coordinates is developed and used to define the actuation forces that can be used in the case of small-deformation problems.
(3) A new procedure for computing the actuation forces from the solution of the FFR inverse-dynamics problem is introduced in Sec. 5. The two approaches of *partially constrained* and *fully constrained inverse dynamics* are defined. The fully constrained inverse dynamics (FCID) can be used for motion and shape control and will be subject of future investigations. The partially constrained inverse dynamics (PCID), used in this investigation, allows for motion control only while maintaining the forward-dynamics oscillations within the inverse-dynamics limits.
(4) The control-actuation approach developed in this study is verified in Sec. 6 using a benchmark mechanism example that has a flexible link. In the numerical verification study, the driving constraint forces predicted using the algorithm developed in this investigation are compared with results previously published in the literature.
(5) To demonstrate the formulation of the control forces using the proposed joint/deformation actuation approach, piezoelectric actuation forces based on the inverse-dynamics solution are developed in Sec. 7, in which a control law that combines conventional articulated-joint and deformation PZT actuation is defined. The *conventional joint actuation* contributes to controlling the joint variables, while the PZT actuation controls the amplitude of the deformation modes and keeps the forward-dynamics oscillations within their inverse-dynamics limits. The procedure described in Sec. 7 leads to a new set of algebraic equations that can be solved for the PZT voltages and the conventional joint actuation forces. This procedure is used to evaluate the effect of the *deformation actuation* often neglected in the design of robot systems.
(6) Implementation of the small-deformation FFR actuation-force approach developed in this study is demonstrated using a two-link flexible robot. The robot end-effector motion is specified, and the joint and PZT actuation moments are calculated. The results obtained using the inverse and forward dynamics are compared in Sec. 8

These results demonstrate deterioration in the robot precision by relying only on the joint actuation and not considering the deformation actuation. Section 9 presents summary and conclusions drawn from this study.

While the literature includes a large number of investigations on the inverse and forward dynamics and control of flexible-robot systems [2,60–62], this paper differs from previous investigations by making the specific contributions summarized above and using the concept of the FFR equipollent systems of forces to define physically meaningful actuation forces with clear interpretation. This defines a new hybrid articulated-joint/deformation actuation approach consistent with the FE/FFR reference conditions that can lead to different definitions of the deformations with respect to the selected body coordinate system and to different FFR forces associated with the deformation modes.

3 Generalized Modal Forces

Nonlinear dynamics of flexible robots with an infinite number of degrees of freedom makes flexible-robot control more complicated. Different flexible-body models are proposed for flexible robots based on different assumptions and requirements [63–69]. In this section, the FFR kinematic equations, used in this study, are summarized and used to define the generalized forces associated with the deformation modes. In the case of flexible bodies, a force acting at a point is equipollent to a system of forces that consist of the same force, a moment that depends on the body deformation, and a set of generalized forces associated with the modal coordinates. A review of the literature of robotic systems reveals that the forces associated with the FE/FFR deformation coordinates have not been considered when developing robot actuation. Therefore, one of the main objectives of this study is to use the modal-force expressions to define physically meaningful material-point and/or rotation-axis actuations.

3.1 Kinematic Equations. In the FFR formulation, the motion of the flexible body is described using two sets of coordinates: the reference and elastic coordinates. The reference coordinates define the location and orientation of the body coordinate system $X_1^i X_2^i X_3^i$ with respect to the global coordinate system $X_1 X_2 X_3$, as shown in Fig. 1. The elastic coordinates are used to define the body deformation with respect to the body coordinate system. Using these coordinates, the global position of an arbitrary point on the body can be written as [70]

$$\mathbf{r}^i = \mathbf{R}^i + \mathbf{A}^i(\bar{\mathbf{u}}_o^i + \bar{\mathbf{u}}_f^i) = \mathbf{R}^i + \mathbf{A}^i(\bar{\mathbf{u}}_o^i + \mathbf{S}^i\mathbf{q}_f^i) \tag{1}$$

In this equation, $\mathbf{R}^i$ is the global position of the body reference point, $\mathbf{A}^i$ is the matrix that defines the orientation of the body coordinate system, $\bar{\mathbf{u}}_o^i = \mathbf{x} = \begin{bmatrix} x_1 & x_2 & x_3 \end{bmatrix}^T$ is the constant position vector of the arbitrary point before deformation with respect to the body coordinate system, $\bar{\mathbf{u}}_f^i = \mathbf{S}^i\mathbf{q}_f^i$ is the deformation vector, $\mathbf{S}^i = \mathbf{S}^i(\mathbf{x})$ is a shape function matrix, and $\mathbf{q}_f^i$ is the vector of elastic coordinates that define the body deformation with respect to its reference. A virtual change in the position vector of the arbitrary point leads to

$$\delta\mathbf{r}^i = \delta\mathbf{R}^i - \mathbf{A}^i\tilde{\bar{\mathbf{u}}}^i\bar{\mathbf{G}}^i\delta\boldsymbol{\theta}^i + \mathbf{A}^i\mathbf{S}^i\delta\mathbf{q}_f^i = \mathbf{L}^i\delta\mathbf{q}^i \tag{2}$$

In this equation, $\tilde{\bar{\mathbf{u}}}^i$ is the skew symmetric matrix associated with the vector $\bar{\mathbf{u}}^i = \bar{\mathbf{u}}_o^i + \bar{\mathbf{u}}_f^i$, $\bar{\mathbf{G}}^i$ is the matrix that relates the angular velocity vector $\bar{\boldsymbol{\omega}}^i$, defined in the body coordinate system, to the time derivatives of the orientation parameters $\boldsymbol{\theta}^i$, that is $\bar{\boldsymbol{\omega}}^i = \bar{\mathbf{G}}^i\dot{\boldsymbol{\theta}}^i$, and

$$\mathbf{L}^i = \begin{bmatrix} \mathbf{I} & -\mathbf{A}^i\tilde{\bar{\mathbf{u}}}^i\bar{\mathbf{G}}^i & \mathbf{A}^i\mathbf{S}^i \end{bmatrix}, \quad \mathbf{q}^i = \begin{bmatrix} \mathbf{R}^{iT} & \boldsymbol{\theta}^{iT} & \mathbf{q}_f^{iT} \end{bmatrix}^T \tag{3}$$

While forces associated with the FFR coordinates may lack a clear physical interpretation because of using the *floating frame*, the FFR kinematic equations can be used to formulate actuation forces that have clear physical interpretations, as demonstrated in this study.

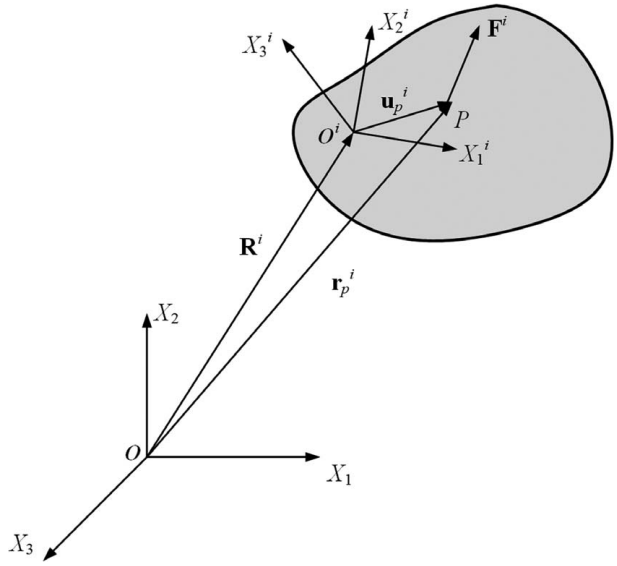

Fig. 1 Spatial rigid body

3.2 Generalized Modal Forces. Using the virtual displacement of the arbitrary point, the virtual work of a force vector $\mathbf{F}^i$ acting at the arbitrary point, as shown in Fig. 1, can be written as

$$\begin{aligned}\delta W_e^i &= \mathbf{F}^{iT}\delta\mathbf{r}^i = \mathbf{F}^{iT}\delta\mathbf{R}^i - \mathbf{F}^{iT}\mathbf{A}^i\tilde{\bar{\mathbf{u}}}^i\bar{\mathbf{G}}^i\delta\boldsymbol{\theta}^i + \mathbf{F}^{iT}\mathbf{A}^i\mathbf{S}^i\delta\mathbf{q}_f^i \\ &= \mathbf{Q}_R^{iT}\delta\mathbf{R}^i + \mathbf{Q}_\theta^{iT}\delta\boldsymbol{\theta}^i + \mathbf{Q}_f^{iT}\delta\mathbf{q}_f^i\end{aligned} \tag{4}$$

where $\mathbf{Q}_R^i = \mathbf{F}^i$, $\mathbf{Q}_\theta^i = \bar{\mathbf{G}}^{iT}\tilde{\bar{\mathbf{u}}}^{iT}\mathbf{A}^{iT}\mathbf{F}^i$, and $\mathbf{Q}_f^i = \mathbf{S}^{iT}\mathbf{A}^{iT}\mathbf{F}^i$. It is clear from the definition of the virtual work that in flexible-body dynamics, the force is no longer a *sliding vector* as in the case of rigid-body dynamics. Furthermore, a force $\mathbf{F}^i$ acting at a point is equipollent to a system of forces that consist of the same force, a deformation-dependent moment, and a set of generalized forces associated with the modal coordinates. The generalized modal forces are associated with modes that describe the overall body deformation and are not associated with discrete physical material points at which the actuators can be placed. These modal forces cannot be ignored in the robot design and control because link deformations absorb energy. It is, therefore, important to replace the system of forces given in the FFR equations with another equipollent system that consists of forces and/or moments associated with material points and motor axes, respectively.

3.3 Actuation Points. There is an infinite number of arrangements for the body floating frame of reference with respect to which the body deformation is defined. Because deformations are relative measures, the generalized forces previously obtained in this section may lack a physical meaning and may not be used directly in the control of robots and mechanisms that consist of deformable bodies. In case of rigid-body dynamics, the body coordinate system is rigidly attached to a material point, and therefore, the forces obtained have a clear physical interpretation. In case of flexible-body dynamics, on the other hand, the generalized forces may not have such a clear interpretation because of the fact that deformations are relative measures. In order to define forces that have clear physical interpretation, the system of forces obtained in this section is converted to another equipollent system of forces and moments associated with coordinates of points and/or axes, as previously mentioned. This is accomplished in the

following section by using the absolute coordinates of a set of discrete points, referred to in this paper as the *actuation points*, whose position coordinates can be determined using the FFR coordinates. In a later section of this paper, it is shown how to replace the FFR generalized forces with joint and piezoelectric moments.

4 Actuation Forces

In the FFR formulation, one set of reference coordinates $\mathbf{q}_r^i = \left[\mathbf{R}^{i^T}\ \boldsymbol{\theta}^{i^T}\right]^T$ is used for the entire body with a set of elastic physical or modal coordinates $\mathbf{q}_f^i$ that define the body deformation relative to its reference. The use of one point and a set of modes does not allow developing an effective control strategy to achieve the desired motion. This challenge can be addressed by transforming the FFR forces to another equipollent system of forces associated with position coordinates. It is assumed that the FFR actuation forces $(\mathbf{Q}_R^i)_a$, $(\mathbf{Q}_\theta^i)_a$, and $(\mathbf{Q}_f^i)_a$ associated, respectively, with the FFR coordinates $\mathbf{R}^i$, $\boldsymbol{\theta}^i$, and $\mathbf{q}_f^i$ are known from the solution of the FFR inverse-dynamics problem in which the desired motion trajectories are specified.

Considering a set of n_p actuation points for the flexible body i and assuming that the unknown actuation force vector at an actuation point k is $\mathbf{F}^{ik}$, one can write the virtual work

$$\delta W_a^i = \sum_{k=1}^{n_p} \mathbf{F}^{ik^T} \delta \mathbf{r}^{ik} = \left[\sum_{k=1}^{n_p} \mathbf{F}^{ik^T} \mathbf{L}^{ik}\right] \delta \mathbf{q}^i \tag{5}$$

where $\mathbf{r}^{ik} = \mathbf{R}^i + \mathbf{A}^i(\bar{\mathbf{u}}_o^{ik} + \bar{\mathbf{u}}_f^{ik})$ is the global position vector of the actuation point expressed in terms of the FFR generalized coordinates, and $\mathbf{L}^{ik}$ is the matrix $\mathbf{L}^i$ evaluated at the actuation point k. The virtual work of the preceding equation must be equal to the virtual work of the generalized actuation forces obtained from the solution of the inverse-dynamics problems, that is

$$\left[\sum_{k=1}^{n_p} \mathbf{F}^{ik^T} \mathbf{L}^{ik}\right] \delta \mathbf{q}^i = \mathbf{Q}_a^{i^T} \delta \mathbf{q}^i \tag{6}$$

where $\mathbf{Q}_a^i = \left[(\mathbf{Q}_R^i)_a^T \quad (\mathbf{Q}_\theta^i)_a^T \quad (\mathbf{Q}_f^i)_a^T\right]^T$ is the vector of generalized actuation forces computed using the inverse-dynamics procedure, as explained in the following section. Because the elements of the vector $\mathbf{q}^i$ in the augmented Lagrangian formulation can be treated as independent, one has $\sum_{k=1}^{n_p} \mathbf{F}^{ik^T} \mathbf{L}^{ik} = \mathbf{Q}_a^i$. The vector on the left-hand side of this equation can be written as

$$\sum_{k=1}^{n_p} \mathbf{L}^{ik^T} \mathbf{F}^{ik} = \left[\mathbf{L}^{i1^T} \quad \mathbf{L}^{i2^T} \quad \cdots \quad \mathbf{L}^{in_p^T}\right] \begin{bmatrix} \mathbf{F}^{i1} \\ \mathbf{F}^{i2} \\ \vdots \\ \mathbf{F}^{in_p} \end{bmatrix} = \mathbf{L}_m^i \mathbf{F}_a^i \tag{7}$$

where

$$\mathbf{L}_m^i = \left[\mathbf{L}^{i1^T} \quad \mathbf{L}^{i2^T} \quad \cdots \quad \mathbf{L}^{in_p^T}\right], \quad \mathbf{F}_a^i = \left[\mathbf{F}^{i1^T} \quad \mathbf{F}^{i2^T} \quad \cdots \quad \mathbf{F}^{in_p^T}\right]^T \tag{8}$$

It follows that

$$\mathbf{L}_m^i \mathbf{F}_a^i = \mathbf{Q}_a^i \tag{9}$$

This system of algebraic equations can be solved for the actuation force vector $\mathbf{F}_a^i$ as

$$\mathbf{F}_a^i = (\mathbf{L}_m^{i^T} \mathbf{L}_m^i)^{-1} \mathbf{L}_m^{i^T} \mathbf{Q}_a^i \tag{10}$$

These actuation forces at the n_p actuation points can be used as input in a forward-dynamics algorithm in order to evaluate the effectiveness of the control strategy. The number of coordinates of the actuation points can be selected equal to the number of coordinates of the flexible body when solving the inverse-dynamics problem. This ensures that the coefficient matrix $\mathbf{L}_m^i$ in Eq. (9) is a square matrix, and in this case, there is no need to multiply Eq. (9) by the transpose of $\mathbf{L}_m^i$. Furthermore, actuation points must be selected such that the coefficient matrix $\mathbf{L}_m^i$ or $\mathbf{L}_m^{i^T}\mathbf{L}_m^i$ in the preceding equations is nonsingular. In the case of the forward-dynamics problem, on the other hand, the number of coordinates of the actuation points does not have to be equal to the number of the flexible-body coordinates.

5 Floating Frame of Reference Inverse-Dynamics Problems

In the inverse-dynamics problem, the desired motion trajectories are specified using a set of algebraic constraint equations. The dynamic equations can be formulated and solved considering these algebraic equations to determine the driving (actuation) forces that produce the desired motion. In case of robot manipulators that consist of rigid bodies, the number of algebraic equations is often equal to the number of the robot degrees of freedom. In this case of rigid-body dynamics, one obtains a set of algebraic equations which can be solved for the accelerations and the actuation forces and torques. There is no need in this case to perform numerical integration of the system differential equations of motion.

In the case of flexible-body dynamics, on the other hand, deformable bodies have deformation degrees of freedom introduced using approximation methods. Using a large number of actuators may not be economically or design feasible. Furthermore, in many applications of robots that consist of flexible links, the focus is on obtaining desired motion trajectories and reducing the vibration to achieve the required precision. As will be discussed in this section, these requirements do not necessarily lead to the conventional inverse-dynamics problem in which only algebraic equations are solved for the actuation forces. As explained below, the inverse-dynamics problem may require numerical integration of a system of differential/algebraic equations (DAEs) if the number of specified motion-trajectory constraint equations is less than the number of the system degrees of freedom. Therefore, in flexible-body dynamics, distinction is made between *motion control* and *motion/shape control*.

5.1 Partially- and Fully Constrained Inverse Dynamics.

In the case of *motion control*, the desired end-effector motion trajectories are specified in the inverse-dynamics problem. Because of the deformation degrees of freedom, the number of motion constraint equations is less than the number of the system coordinates. This is the case of *partially constrained inverse dynamics* (PCID), which requires using direct numerical integration to determine the driving constraint forces. In the PCID approach, despite the fact that no constraints are imposed on the deformation coordinates, the solution of the FFR inverse problem leads to driving constraint forces associated with the reference and elastic coordinates. The driving constraint forces associated with the elastic coordinates cannot be ignored if the link oscillations in the forward-dynamics problem are to remain within the inverse-dynamics limits.

In case of *motion/shape control*, all the degrees of freedom are prescribed, including the deformation degrees of freedom. In this case, the number of specified motion-trajectory constraint equations is equal to the number of system degrees of freedom. While in this case the number of constraint equations is increased to impose constraints on the deformation shape to suppress the vibration, this case of *fully constrained inverse dynamics* (FCID) leads to a system of algebraic equations which can be solved for the accelerations and driving constraint forces. In this FCID case, there is no need for using direct numerical integration methods since the solution of the resulting system of the algebraic equation provides the information needed for developing the control-actuation strategy. This investigation is concerned with the motion control which can be addressed using the PCID approach.

5.2 Specified Motion-Trajectory Constraints. In general, the specified motion-trajectory and any other performance-criteria constraints can be formulated using a set of algebraic constraint equations which can be written in a vector form as $\mathbf{C}_s(\mathbf{q}, t) = \mathbf{0}$, where $\mathbf{q}$ is the vector of the system coordinates that include the rigid-body and flexible-body reference and deformation coordinates. The constraint equations $\mathbf{C}_s(\mathbf{q}, t) = \mathbf{0}$ can be of the rheonomic (explicit function of time) type. Other constraint equations that define mechanical joints of the articulated robot systems are denoted as $\mathbf{C}_m(\mathbf{q}, t) = \mathbf{0}$. Therefore, the total vector of algebraic constraint equations can be written as $\mathbf{C}(\mathbf{q}, t) = \begin{bmatrix} \mathbf{C}_s^T & \mathbf{C}_m^T \end{bmatrix}^T = \mathbf{0}$.

5.3 Generalized Actuation Forces. The system algebraic constraint equations, including the specified motion-trajectory and performance-criteria constraints, can be combined with the system differential equations of motion to form a differential/algebraic equation (DAE) system using the technique of Lagrange multipliers. Lagrange multipliers and the constraint Jacobian matrix can be used to determine the generalized constraint forces associated with the reference and elastic coordinates of the flexible bodies. The system differential equations of motion can be written as $\mathbf{M}\ddot{\mathbf{q}} = \mathbf{Q}_e + \mathbf{Q}_c$, where $\mathbf{M}$ is the system symmetric and nonlinear mass matrix in the case of the FFR formulation, $\mathbf{Q}_e$ is the vector of applied and quadratic-velocity inertia forces, and $\mathbf{Q}_c$ is the vector of constraint forces written in terms of Lagrange multipliers as

$$\mathbf{Q}_c = -\mathbf{C}_{\mathbf{q}}^T\boldsymbol{\lambda} = -\mathbf{C}_{s\mathbf{q}}^T\boldsymbol{\lambda}_s - \mathbf{C}_{m\mathbf{q}}^T\boldsymbol{\lambda}_m = -\begin{bmatrix} \mathbf{C}_{s\mathbf{q}}^T & \mathbf{C}_{m\mathbf{q}}^T \end{bmatrix}\begin{bmatrix} \boldsymbol{\lambda}_s \\ \boldsymbol{\lambda}_m \end{bmatrix} \tag{11}$$

In this equation, $\mathbf{C}_{\mathbf{q}} = \partial\mathbf{C}/\partial\mathbf{q} = \begin{bmatrix} \mathbf{C}_{s\mathbf{q}}^T & \mathbf{C}_{m\mathbf{q}}^T \end{bmatrix}^T$ is the constraint Jacobian matrix; $\boldsymbol{\lambda} = \begin{bmatrix} \boldsymbol{\lambda}_s^T & \boldsymbol{\lambda}_m^T \end{bmatrix}^T$ is the vector of Lagrange multipliers; $\mathbf{C}_{s\mathbf{q}} = \partial\mathbf{C}_s/\partial\mathbf{q}$ and $\mathbf{C}_{m\mathbf{q}} = \partial\mathbf{C}_m/\partial\mathbf{q}$ are, respectively, the Jacobian matrices of the constraint equations $\mathbf{C}_s$ and $\mathbf{C}_m$; and $\boldsymbol{\lambda}_s$ and $\boldsymbol{\lambda}_m$ are Lagrange multipliers associated, respectively, with the constraint equations $\mathbf{C}_s$ and $\mathbf{C}_m$. The constraint equations at the acceleration level is defined by differentiating the constraints twice with respect to time as

$$\mathbf{C}_{\mathbf{q}}\ddot{\mathbf{q}} = \begin{bmatrix} \mathbf{C}_{s\mathbf{q}} \\ \mathbf{C}_{m\mathbf{q}} \end{bmatrix}\ddot{\mathbf{q}} = \begin{bmatrix} \mathbf{Q}_{ds} \\ \mathbf{Q}_{dm} \end{bmatrix} \tag{12}$$

where $\mathbf{Q}_{ds}$ and $\mathbf{Q}_{dm}$ are vectors that result from differentiating the constraint equations twice with respect to time and absorb terms which are not linear in the accelerations.

Using the system differential equations of motion, $\mathbf{M}\ddot{\mathbf{q}} = \mathbf{Q}_e + \mathbf{Q}_c$, and the constraint equations at the acceleration level, the augmented form of the equations of motion can be written as

$$\begin{bmatrix} \mathbf{M} & \mathbf{C}_{s\mathbf{q}}^T & \mathbf{C}_{m\mathbf{q}}^T \\ \mathbf{C}_{s\mathbf{q}} & \mathbf{0} & \mathbf{0} \\ \mathbf{C}_{m\mathbf{q}} & \mathbf{0} & \mathbf{0} \end{bmatrix}\begin{bmatrix} \ddot{\mathbf{q}} \\ \boldsymbol{\lambda}_s \\ \boldsymbol{\lambda}_m \end{bmatrix} = \begin{bmatrix} \mathbf{Q}_e \\ \mathbf{Q}_{ds} \\ \mathbf{Q}_{dm} \end{bmatrix} \tag{13}$$

This sparse matrix equation can be solved for the acceleration vector $\ddot{\mathbf{q}}$ and the vectors of Lagrange multipliers $\boldsymbol{\lambda}_s$ and $\boldsymbol{\lambda}_m$. If the number of algebraic constraint equations is not equal to the number of the system degrees of freedom, one has the PCID case that requires numerical integration of the acceleration vector $\ddot{\mathbf{q}}$ to determine the coordinates and velocities. It is necessary, however, to use a numerical algorithm that ensures that the constraint equations are satisfied at the position, velocity, and acceleration levels. To this end, the independent accelerations are identified and integrated forward in time to determine the independent coordinates and velocities. The dependent variables are determined from the algebraic constraint equations and their derivatives. This procedure ensures consistency with the *D'Alembert-Lagrange principle* or the principles upon which accurate numerical integration methods are developed. In the FCID case, on the other hand, the number of algebraic constraint equations is equal to the number of coordinates, and in this case, there is no need for performing numerical integration since the algebraic constraint equations and their derivatives completely define the system coordinates, velocities, and accelerations.

In both PCID and FCID cases, the vectors of Lagrange multipliers $\boldsymbol{\lambda}_s$ and $\boldsymbol{\lambda}_m$ can be used to determine, respectively, the generalized actuation and joint-reaction forces. In particular, for a body i in the system, the driving constraint forces can be evaluated as $\mathbf{Q}_a^i = -\mathbf{C}_{s\mathbf{q}^i}^T\boldsymbol{\lambda}_s$, where $\mathbf{C}_{s\mathbf{q}^i} = \partial\mathbf{C}_s/\partial\mathbf{q}^i$ and $\mathbf{q}^i$ is the vector of generalized coordinates of the FFR body i. The vector of generalized actuation forces $\mathbf{Q}_a^i$ can be used to determine the actuation-force vectors $\mathbf{F}^{ik}$, $k = 1, 2, \ldots, n_p$, at the actuation points, as previously described.

6 Verification of the Proposed Approach

In this section, a benchmark example of a flexible slider-crank mechanism [35] is used to provide verification of the inverse- and forward-dynamics approaches proposed in this study. Figure 2 shows the slider-crank mechanism, which consists of four bodies; the ground (body 1), the crankshaft (body 2), the connecting rod (body 3), and the slider block (body 4). All the links are made of steel and assumed rigid except the connecting rod which is considered flexible. The connecting rod has a length of 0.35 m, a diameter of 0.006 m, a mass density of 7800 kg/m^3, and a modulus of elasticity of 2.0×10^{11} N/m^2. The connecting rod is modeled using the FE method and is divided into four two-dimensional beam elements. The first six modes, with 1% modal damping for all modes, are used in the simulation. The dimensions and properties of the mechanism are shown in Table 1. In the numerical simulation, the motion of the slider block is specified and is defined using the harmonic function $R_x^4 = 0.35 - 0.12\sin(\omega t)$, where R_x^4 is the coordinate of the slider block in the horizontal direction, and $\omega = 100$ rad/s. The simulations of the flexible slider-crank mechanism are performed using the general-purpose MBS software **SIGMA/SAMS** (**S**ystematic **I**ntegration of **G**eometric **M**odeling and **A**nalysis for the **S**imulation of **A**rticulated **M**echanical **S**ystems). The results of the inverse and forward dynamics of the proposed approach are compared with the results presented in the literature [35]. Using the specified motion trajectory, the driving constraint force that produces the desired motion is obtained using the PCID approach. The desired motion of the slider block can then be obtained using an actuator that drives the slider block.

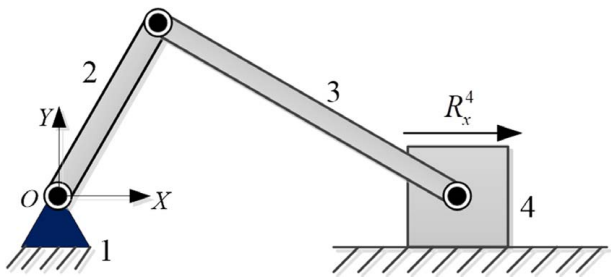

Fig. 2 Planar slider-crank mechanism

Table 1 Slider-crank mechanism dimensions and inertia properties

Link number	Diameter (m)	Length (m)	Mass (kg)
2	0.006	0.15	0.03308
3	0.006	0.35	0.07719
4	–	–	0.1

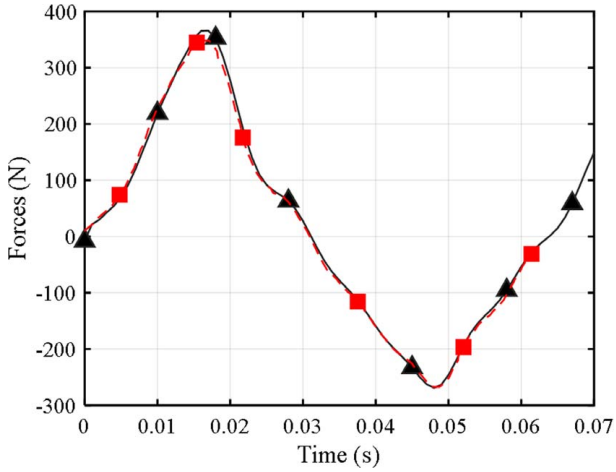

Fig. 3 Actuator force (—■— [35]; —▲— proposed approach)

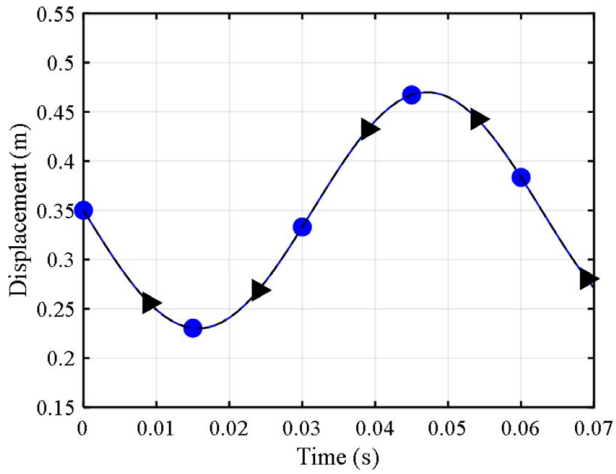

Fig. 4 Motion trajectory of the slider block (—●— Specified motion trajectory; —▲— Desired motion predicted using forward dynamics)

Figure 3 shows the driving constraint force, which is the actuation force predicted using the PCID approach, and it is the force required to achieve the desired motion of the slider block. The results presented in this figure show that the actuation force obtained by the PCID method is in good agreement with the results presented in the literature [35]. Figures 4 and 5 show, respectively, the actual motion trajectory of the slider block and the midpoint transverse deformation of the flexible connecting rod. These results show good agreement with the results reported in the literature [35].

7 Characterization of Joint/Deformation Actuations

In this section, the piezoelectric actuation is used as an example to demonstrate the procedure of using the inverse-dynamics solution to determine the piezoelectric voltages required to produce actuation moments associated with the deformation modes. These actuation moments have a clear physical interpretation regardless of the FFR coordinates which may lack an obvious physical meaning because of the nature of the FFR coordinate system used.

7.1 Piezoelectric Actuators. Using PZT actuators, as the one shown in Fig. 6, actuation moments proportional to the control voltage can be produced using the relationship [71–73]

$$M_{p,k} = c_k V_k(t) \tag{14}$$

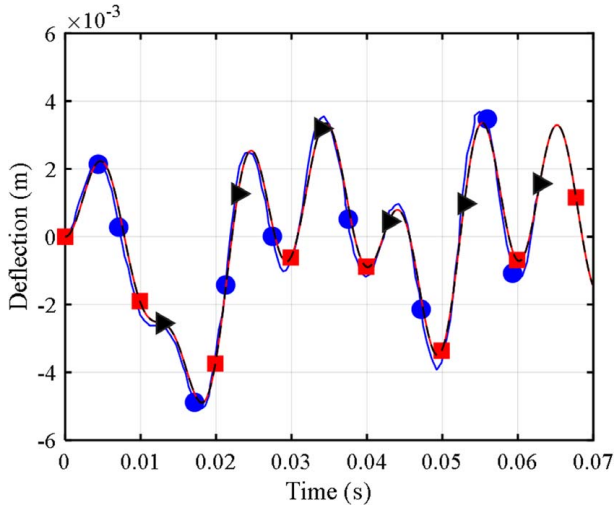

Fig. 5 Midpoint transverse displacement of the connecting rod (—●— [35]; —■— Inverse dynamics results; —▲— Forward-dynamics results)

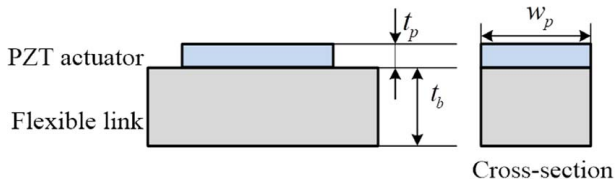

Fig. 6 A flexible link with piezoelectric actuator

where $M_{p,k}$ is the actuation moment; $V_k = V_k(t)$ is the control voltage applied to the kth piezoelectric actuator; subscripts p and k refer, respectively, to piezoelectric and kth piezoelectric actuator, and c_k is a constant which depends on the material and geometric properties of the piezoelectric actuator and represents the actuating moment per unit volt. This constant can be written in terms of the material properties and dimensions of the piezoelectric actuator as $c_k = E_p d_{31} w_p (t_p + t_b)/2$, where E_p is Young's modulus, d_{31} is PZT material constant, w_p and t_p are, respectively, the width and thickness of the PZT actuator, and t_b is the thickness of the flexible link on which the PZT is placed. Therefore, the virtual work of the kth PZT actuator force based on the FFR formulation can be written as $\delta W_{p,k} = M_{p,k}(\delta\theta_{p,k2} - \delta\theta_{p,k1})$, where $\theta_{p,k1}$ and $\theta_{p,k2}$ are the rotation angles of the two ends of the PZT actuator, which can be expressed in terms of the FFR shape function matrix and nodal coordinates of flexible link i. Therefore, $\delta W_{p,k}$ can be written as

$$\delta W^i_{p,k} = M^i_{p,k}(\delta\theta^i_{p,k2} - \delta\theta^i_{p,k1}) = c^i_k V^i_k \boldsymbol{\Phi}^i_{e,k} \delta\mathbf{q}^i_f \tag{15}$$

where $\boldsymbol{\Phi}^i_{e,k} = [\mathbf{S}'(x_{k,2}) - \mathbf{S}'(x_{k,1})]$, $\mathbf{S}$ is the shape function matrix of the flexible link, $\mathbf{S}' = \partial\mathbf{S}/\partial x$, x is the axial coordinate of the flexible link, $x_{k,1}$ and $x_{k,2}$ are the coordinates of the two ends of the PZT actuator, and $\mathbf{q}^i_f$ is the vector of elastic coordinates of the flexible link, which can be written in terms of the vector of modal coordinates $\mathbf{p}^i_f$ as $\mathbf{q}^i_f = \boldsymbol{\Phi}^i_m \mathbf{p}^i_f$, where $\boldsymbol{\Phi}^i_m$ is the modal matrix [70]. Using the virtual change $\delta\mathbf{q}^i_f = \boldsymbol{\Phi}^i_m \delta\mathbf{p}^i_f$, the virtual work of n_{pz} PZT actuators on a flexible link i can be written in terms of the modal coordinates as

$$\delta W^i_{pz} = \left(\sum_{k=1}^{n_{pz}} M^i_{p,k} \boldsymbol{\Phi}^i_{e,k}\right) \boldsymbol{\Phi}^i_m \delta\mathbf{p}^i_f = \left(\sum_{k=1}^{n_{pz}} c^i_k V^i_k \boldsymbol{\Phi}^i_{e,k}\right) \boldsymbol{\Phi}^i_m \delta\mathbf{p}^i_f = \mathbf{F}^{i^T}_{pz} \delta\mathbf{p}^i_f \tag{16}$$

which defines the generalized PZT actuation forces associated with the modal coordinates as

$$\mathbf{F}^i_{pz} = \boldsymbol{\Phi}^{i^T}_m \left(\sum_{k=1}^{n_{pz}} \boldsymbol{\Phi}^{i^T}_{e,k} M^i_{p,k} \right) = \boldsymbol{\Phi}^{i^T}_m \left(\sum_{k=1}^{n_{pz}} \boldsymbol{\Phi}^{i^T}_{e,k} c^i_k V^i_k \right) = \boldsymbol{\Phi}^i_V \mathbf{V}^i \quad (17)$$

In this equation, $\boldsymbol{\Phi}^i_V = \boldsymbol{\Phi}^{i^T}_m \begin{bmatrix} c^i_1 \boldsymbol{\Phi}^{i^T}_{e,1} & c^i_2 \boldsymbol{\Phi}^{i^T}_{e,2} & \cdots & c^i_{n_{pz}} \boldsymbol{\Phi}^{i^T}_{e,n_{pz}} \end{bmatrix}$ and $\mathbf{V}^i = \begin{bmatrix} V^i_1 & V^i_2 & \cdots & V^i_{n_{pz}} \end{bmatrix}^T$ is the vector of the piezoelectric voltage of the flexible body i. This definition of the generalized piezoelectric forces associated with the modal coordinates will be used to define a system of algebraic equations that can be solved for the piezoelectric voltages required to define the PZT actuation moments.

7.2 System Kinematics. Using the FFR coordinate vector $\mathbf{q}^i = \begin{bmatrix} \mathbf{R}^{i^T} & \boldsymbol{\theta}^{i^T} & \mathbf{q}^{i^T}_f \end{bmatrix}^T$ of the flexible body i, exact modeling of the rigid-body dynamics when the structures rotate as rigid bodies can be achieved. When the modal coordinates are used, one can introduce the vector $\mathbf{q}^i_p = \begin{bmatrix} \mathbf{R}^{i^T} & \boldsymbol{\theta}^{i^T} & \mathbf{p}^{i^T}_f \end{bmatrix}^T$ and write $\delta\mathbf{q}^i = \mathbf{D}^i \delta\mathbf{q}^i_p$, where

$$\mathbf{D}^i = \begin{bmatrix} \mathbf{I} & \mathbf{0} \\ \mathbf{0} & \boldsymbol{\Phi}^i_m \end{bmatrix} \quad (18)$$

In this equation, $\mathbf{I}$ is the identity matrix. The vector of generalized coordinates of a system that has n_b bodies can be written as $\mathbf{q} = \begin{bmatrix} \mathbf{q}^{1^T} & \mathbf{q}^{2^T} & \cdots & \mathbf{q}^{n^T_b} \end{bmatrix}^T$. In case of articulated robot system, this vector of coordinates can be written in terms of the vector $\mathbf{q}_p = \begin{bmatrix} \mathbf{q}^{1^T}_p & \mathbf{q}^{2^T}_p & \cdots & \mathbf{q}^{n^T_b}_p \end{bmatrix}^T$ of the Cartesian and elastic degrees of freedom. Using these notations, the virtual change in $\mathbf{q}$ can be written in terms of the virtual change in $\mathbf{q}_p$ as $\delta\mathbf{q} = \mathbf{D}\delta\mathbf{q}_p$, where $\mathbf{D}$ is a block-diagonal matrix whose block-diagonal elements are the matrices $\mathbf{D}^i$ of the bodies. Furthermore, using the system kinematic constraint equations, the vector of Cartesian and modal coordinates $\mathbf{q}_p$ can be written in terms of the vector $\mathbf{q}_{je}$ of the independent joint and elastic modal coordinates as $\delta\mathbf{q}_p = \mathbf{D}_p \delta\mathbf{q}_{je}$, where $\mathbf{D}_p$ is a velocity transformation matrix defined using the kinematic constraint equations of the joints [70]. In this case, one can write the virtual change in the absolute Cartesian and physical elastic coordinates in terms of the virtual change of the system degrees of freedom as

$$\delta\mathbf{q} = \mathbf{D}\delta\mathbf{q}_p = \mathbf{D}\mathbf{D}_p \delta\mathbf{q}_{je} = \mathbf{D}_{je}\delta\mathbf{q}_{je} \quad (19)$$

where $\mathbf{D}_{je} = \mathbf{D}\mathbf{D}_p$ is the velocity transformation matrix that relates the virtual changes of the two vectors $\mathbf{q}$ and $\mathbf{q}_{je}$.

7.3 Piezoelectric Forces. In the FFR formulation, origin of the body coordinate system may not be rigidly attached to a material point on the body. Therefore, the reference coordinates and the elastic coordinates, which define the body deformation with respect to its coordinate system, may lack an obvious physical meaning. In developing a simulation-based control strategy, however, the goal is to define actuation forces that have a clear physical interpretation. The obtained simulation results based on accurate computer models can be used to define parameters that enter into the definition of physically meaningful actuation forces. In case of piezoelectric actuation, the inverse-dynamics results can be systematically used to define the voltage-time history required to produce the desired motion. When this voltage is used, the desired physically meaningful piezoelectric actuation bending moments can be computed as previously mentioned in this section.

Regardless of the reference conditions used in the FFR formulation, the driving control forces $\mathbf{F}_q$ associated with the coordinate vector $\mathbf{q}$ can be obtained using the inverse-dynamics procedure, previously discussed, as $\mathbf{F}_q = -\mathbf{C}^T_{s\mathbf{q}} \boldsymbol{\lambda}_s$, where $\mathbf{C}_{s\mathbf{q}}$ is the Jacobian matrix of the driving constraints, and $\boldsymbol{\lambda}_s$ is the vector of Lagrange multipliers associated with the driving constraints. Knowing the vector $\mathbf{F}_q$, the virtual work can be used to determine the actuation forces $\mathbf{F}_{je}$ associated with the coordinates $\mathbf{q}_{je}$. To this end, one can write

$$\begin{aligned} \delta W_{je} &= \mathbf{F}^T_q \delta\mathbf{q} = (\mathbf{F}^T_q \mathbf{D}_{je}) \delta\mathbf{q}_{je} \\ &= -(\boldsymbol{\lambda}^T_s \mathbf{C}_{s\mathbf{q}} \mathbf{D}_{je}) \delta\mathbf{q}_{je} = \mathbf{F}^T_{je} \delta\mathbf{q}_{je} \end{aligned} \quad (20)$$

where the driving joint and PZT moments are defined using the inverse-dynamics solution as

$$\mathbf{F}_{je} = -\mathbf{D}^T_{je} \mathbf{C}^T_{s\mathbf{q}} \boldsymbol{\lambda}_s \quad (21)$$

This equation can be used to define the actuation joint and PZT moment equations.

7.4 Algebraic Joint-Moment and Voltage Equations. The actuation forces can be classified as an *articulated joint force and moments* defined by the vector $\mathbf{F}_{aj}$ associated with the articulated joint degrees of freedom $\mathbf{q}_{aj}$ and *piezoelectric moments* $\mathbf{F}_{pz}$ associated with the modal coordinates $\mathbf{q}_{pz}$ which can represent all or a subset of the system modal coordinate vector $\mathbf{p}_f$. The vector $\mathbf{F}_{pz}$ is the assembly of the vectors $\mathbf{F}^i_{pz}$, $i = 1, 2, \ldots, n_b$, defined previously in this section in terms of the PZT voltages as $\mathbf{F}^i_{pz} = \boldsymbol{\Phi}^{i^T}_m \left(\sum_{k=1}^{n_{pz}} \boldsymbol{\Phi}^T_{e,k} c^i_k V^i_k \right) = \boldsymbol{\Phi}^i_V \mathbf{V}^i$. Using this equation and using the notation of the *system voltage vector* $\mathbf{V} = \begin{bmatrix} \mathbf{V}^{1^T} \mathbf{V}^{2^T} \cdots \mathbf{V}^{n^T_b} \end{bmatrix}^T$, the vector $\mathbf{F}_{pz}$ can be written as

$$\begin{aligned} \mathbf{F}_{pz} &= \begin{bmatrix} \mathbf{F}^{1^T}_{pz} & \mathbf{F}^{2^T}_{pz} & \cdots & \mathbf{F}^{n^T_b}_{pz} \end{bmatrix}^T \\ &= \begin{bmatrix} \boldsymbol{\Phi}^1_V & \boldsymbol{\Phi}^2_V & \cdots & \boldsymbol{\Phi}^{n_b}_V \end{bmatrix} \begin{bmatrix} \mathbf{V}^1 \\ \mathbf{V}^2 \\ \vdots \\ \mathbf{V}^{n_b} \end{bmatrix} = \boldsymbol{\Phi}_V \mathbf{V} \end{aligned} \quad (22)$$

Using these definitions, the virtual work of the actuation forces can be written in a different form as $\delta W_{je} = \mathbf{F}^T_{je} \delta\mathbf{q}_{je} = \mathbf{F}^T_{aj} \delta\mathbf{q}_{aj} + \mathbf{F}^T_{pz} \delta\mathbf{q}_{pz}$, where in this equation $\mathbf{q}_{je} = \begin{bmatrix} \mathbf{q}^T_{aj} & \mathbf{q}^T_{pz} \end{bmatrix}^T$. Because the vector $\mathbf{F}_{je}$ can be computed from the inverse-dynamics solution, the definition of the virtual work $\delta W_{je} = \mathbf{F}^T_{je} \delta\mathbf{q}_{je} = \mathbf{F}^T_{aj} \delta\mathbf{q}_{aj} + \mathbf{F}^T_{pz} \delta\mathbf{q}_{pz}$ leads to the following system of algebraic equations:

$$\begin{bmatrix} \mathbf{I} & \mathbf{0} \\ \mathbf{0} & \boldsymbol{\Phi}_V \end{bmatrix} \begin{bmatrix} \mathbf{F}_{aj} \\ \mathbf{V} \end{bmatrix} = \mathbf{F}_{je} \quad (23)$$

This system can be solved at every time-step in order to determine the joint actuation forces and/or moments, and the PZT voltages required to define the PZT actuation moments.

8 Numerical Results

In this section, the two-link flexible-robot manipulator system as shown in Fig. 7 is used to demonstrate the proposed joint/deformation actuation and control approach. The model, which consists of two flexible links, has two revolute joints: one connects the first flexible link to the ground, and the second connects the first and second flexible links. In this example, the manipulator is assumed to move in *XY*-plane and the goal is to control the end-effector motion using two motors placed at the two joints, and PZT actuators

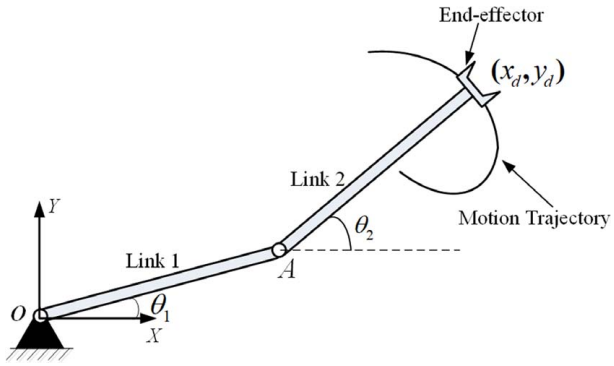

Fig. 7 Two-link flexible-robot manipulator

distributed along the length of each flexible link. As previously discussed, the flexible MBS motion cannot be controlled by simply providing actuation-force inputs equal to the number of the joint degrees of freedom. The uncontrolled elastic degrees of freedom can induce instability and undesirable oscillations, and therefore, it is necessary to provide actuation forces associated with the deformation modes [35]. Therefore, in this study, motors at the joints and PZT actuators bonded on the flexible links are used to control both the joint and elastic displacements. In this study, the number of PZT actuators of each flexible link is equal to the number of the link elastic coordinates. This choice allows using a number of force inputs equal to the number of degrees of freedom and ensures that the coefficient matrix in Eq. (23) is a square matrix. The virtual work of the actuating moments can be considered as a special case of the more general expression previously developed and can be written as

$$\delta W_{je} = M_\theta^1 \delta\theta_1 + M_\theta^2 \delta\theta_2 + \sum_{k=1}^{n_{pz1}} M_{p,k}^1 \mathbf{\Phi}_{e,k}^1 \mathbf{\Phi}_m^1 \delta \mathbf{p}_f^1 + \sum_{k=1}^{n_{pz2}} M_{p,k}^2 \mathbf{\Phi}_{e,k}^2 \mathbf{\Phi}_m^2 \delta \mathbf{p}_f^2 \tag{24}$$

where M_θ^l. $l = 1, 2$, are the articulated-joint actuation moments; and n_{pz1} and n_{pz2} are, respectively, the number of piezoelectric actuators of the first and second links.

8.1 Model Data. Table 2 shows the dimensions and inertia properties of the two-link robot considered in the numerical investigation. Each link is divided into 20 Euler–Bernoulli beam elements, and in the dynamic simulation model, simply-supported and cantilever reference conditions are used for the first link and second link, respectively. For each link, ten modal coordinates are used. The elastic modulus is assumed 2.068427×10^{11} N/m^2, and the density is 7850 kg/m^3. The initial configuration of links 1 and 2 are, respectively, defined by the angles $\theta_1 = 0$ and $\theta_2 = \pi/3$. The gravity effect is considered using the gravity constant $g = 9.81$ m/s^2. The motion of the end-effector is specified according to $x_d(t) = x_0 \cos(\pi t/4)$, $y_d(t) = y_0 \cos(\pi t/4)$. The simulations are performed using the general-purpose MBS software **SIGMA/SAMS**.

8.2 Motion and Force Results. The simulation results of the motion trajectory of the end-effector are presented in Fig. 8,

Table 2 Two-link robot dimensions and inertia properties

Link number	Length (m)	Cross section	Mass (kg)	Mass moment of inertia (kg · m^2)
1	1	0.025 m × 0.015 m	2.94375	0.2453125
2	1	0.025 m × 0.015 m	2.94375	0.98125

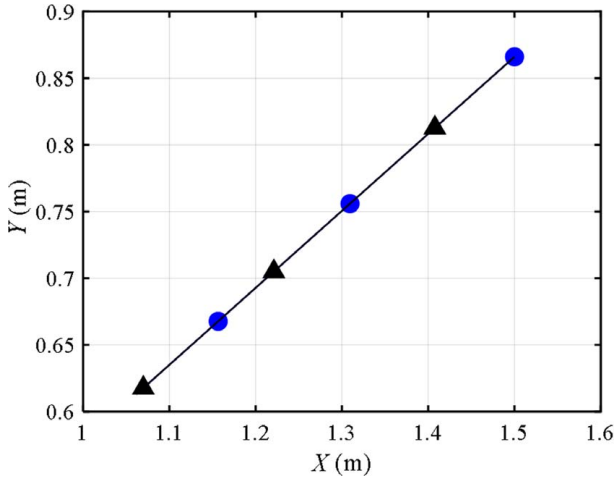

Fig. 8 Motion trajectory of the end-effector (—●— Specified motion trajectory; —▲— Desired motion from forward dynamics)

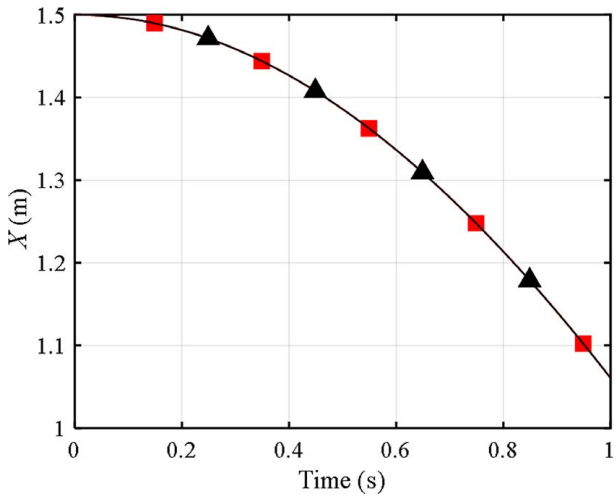

Fig. 9 Global *X*-coordinate of the end-effector (—■— Inverse dynamics; —▲— Forward dynamics)

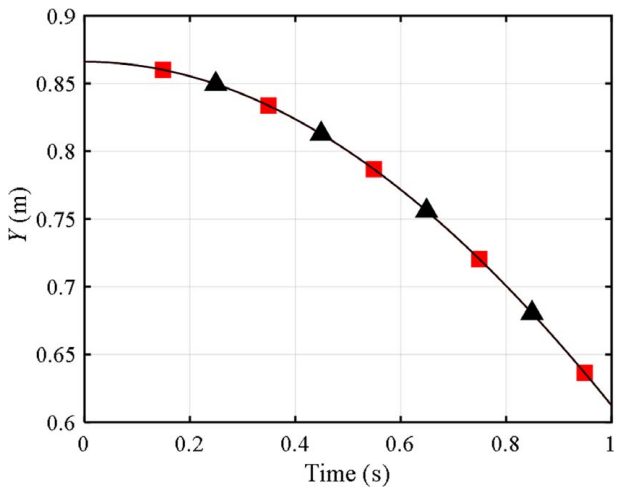

Fig. 10 Global *Y*-coordinate of the end-effector (—■— Inverse dynamics; —▲— Forward dynamics)

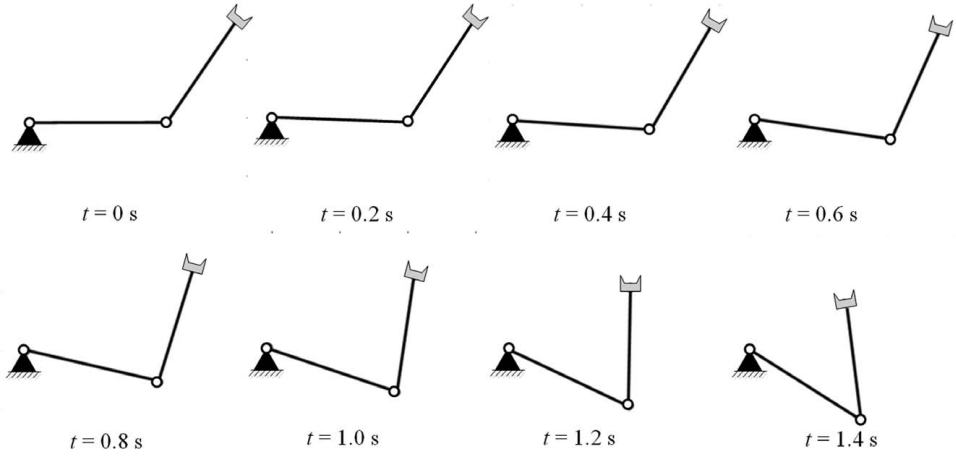

Fig. 11 Robot configurations at different time points

which shows the desired specified trajectory x_d and y_d as well as the end-effector motion predicted using the forward dynamics based on driving forces determined using the PCID approach. The results shown in Fig. 8 demonstrate that the forward-dynamics motion trajectory is in good agreement with the desired trajectories. The results of the global coordinates of the end-effector presented in Figs. 9 and 10 show also good agreement between the solutions of the inverse and forward dynamics. Figure 11 shows the motion of the planar robot at selected time points. Figures 12 and 13 show that the transverse deformations of flexible links 1 and 2 obtained using the inverse and forward dynamics are in good agreement; demonstrating that the application of the joint and deformation actuation driving moments does not lead to a noticeable increase in the link oscillations. The *joint actuation* moments at joints *O* and *A* are shown in Fig.14.

8.3 Piezoelectric Voltages. The parameters of piezoelectric materials selected are shown in Table 3 [72]. In this example, 10 PZT actuators are used for each flexible link to control the 10 modes in the forward-dynamics simulation. The control voltages of the PZT actuator arrangement are shown in Figs. 15 and 16, which show volt oscillations due to the link deformations, a behavior consistent with results reported in the literature [46,47,73–76]. Normally, the PZT actuators can generate large forces with relatively small voltage [72]. For practical considerations, the control voltages of the PZT actuators are limited to ±200 V [73]. It should be noted that different numbers and locations of the piezoelectric actuators can lead to different control voltages [77,78]. The approach proposed in this work can be used to determine the

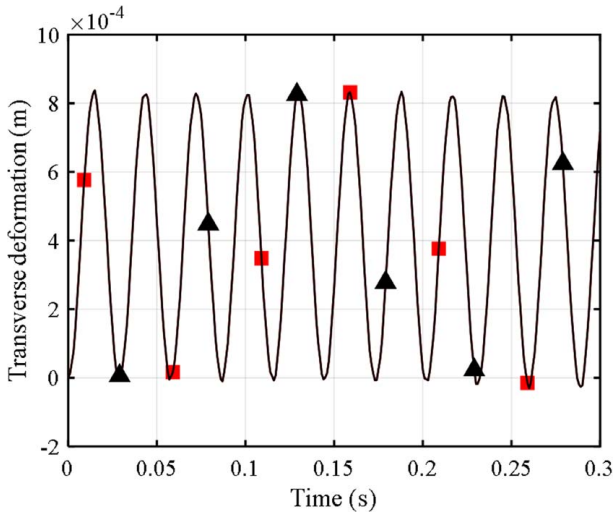

Fig. 13 Transverse deformation of the end-effector of link 2 (—■— Inverse dynamics; —▲— Forward dynamics)

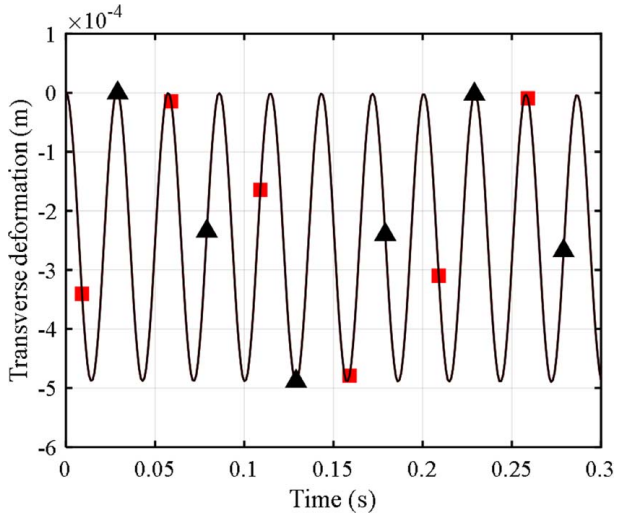

Fig. 12 Transverse deformation of the midpoint of link 1 (—■— Inverse dynamics; —▲— Forward dynamics)

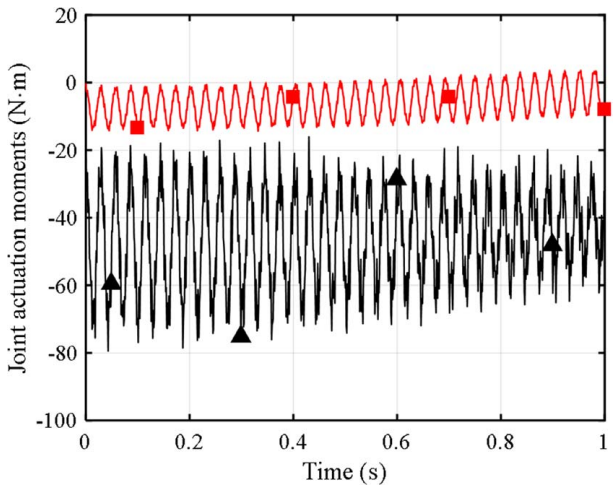

Fig. 14 Joint actuation moments (—▲— Joint *O* and —■— Joint *A*)

Table 3 Parameters of piezoelectric (PZT) material

Parameters	Values
Modulus	63 GPa
Length	0.05 m
Thickness	0.75 mm
Width	0.025 m
Density	7600 kg/m^3
d_{31}	110×10^{-12} m/V

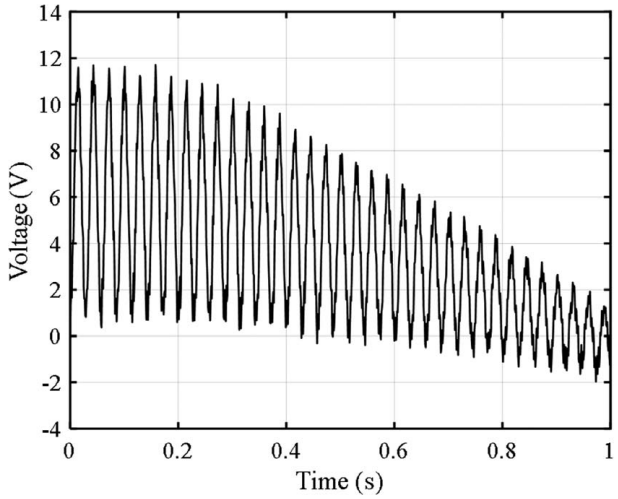

Fig. 15 Control voltage for the PZT actuator on the flexible link 1

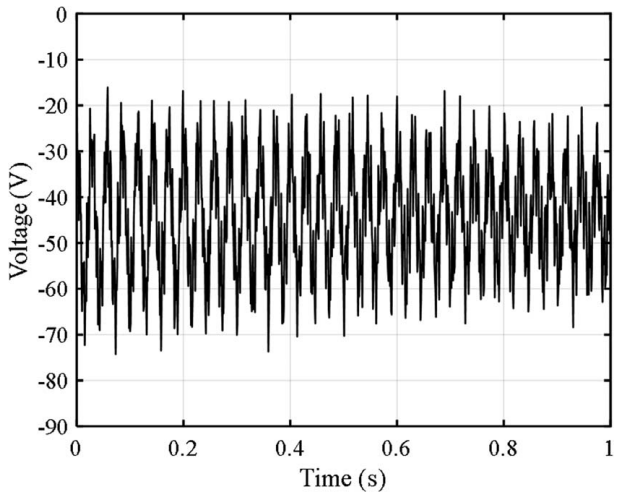

Fig. 16 Control voltage for the PZT actuator on the flexible link 2

piezoelectric control voltages required to achieve the desired motion trajectories. Future investigations will be focused on studying the optimum numbers and locations of PZT actuators and their effect on power consumption. Figure 17 shows the solution obtained when the piezoelectric deformation actuation is not applied and only the joint actuation is used. The results presented in this figure demonstrate a significant increase in the amplitude of vibration of the end effector when relying only on the joint actuation without consideration of the deformation actuations.

8.4 Efficiency of the PCID and FCID Procedures. It is to be noted that the efficiency of the PCID procedure depends on the

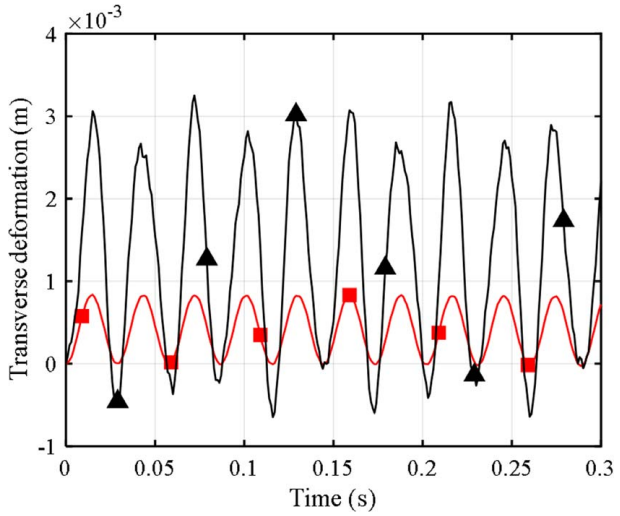

Fig. 17 Transverse deformation of end-effector (—■— Inverse dynamics; —▲— Forward dynamics without PZT actuators)

number of uncontrolled elastic modes in the model because they represent the degrees of freedom whose second derivatives must be integrated. In the case of the FCID procedure, on the other hand, none of the elastic accelerations is integrated, and therefore, the FCID problem is reduced to solving a system of algebraic equations that can be used to determine the actuation forces. This latter case is very efficient, as previously noted, since it does not require numerical integration and can be used for both motion and shape control [79].

The computer simulations were performed in this investigation using an Intel(R) Xeon(R) CPU E5-1650 0@3.20 GHZ computer. The CPU time for the partially constrained inverse-dynamics problem used to determine the actuation forces was found to be 13 s. The use of fully constrained inverse-dynamics problem for the motion and shape control of the flexible-robot system can lead to a significant reduction in the CPU time, as previously explained since only solving algebraic equations is required.

9 Summary and Conclusions

The inverse-dynamics procedure for flexible-robot manipulators leads to driving forces associated with the deformation modes. These forces, which have been ignored in developing actuations of flexible robots, may lack clear physical interpretation because of the nature of the coordinates used in the FFR formulation. A literature survey has shown that there is no computational procedure in existence that can be used to convert these FFR driving forces to actuation forces that have clear physical meaning. This paper addresses this fundamental issue by introducing a new computational joint/deformation actuation approach for the *motion control* of flexible-robot manipulators. The goal is to ensure that the desired motion trajectories are achieved while the flexible link oscillations remain within the inverse-dynamics boundaries. As discussed in the paper, two approaches can be considered in order to determine the actuation forces required to achieve the desired motion trajectories; the PCID and FCID approaches. The FCID approach will be considered in future investigations to achieve *motion and shape controls*, while the PCID approach, considered in this study, allows achieving the desired motion trajectories, determining systematically the actuation forces and moments associated with the joint and elastic degrees of freedom and avoiding deteriorations in the vibration characteristics as measured by the inverse-dynamics solutions. The procedure for determining the actuation forces associated with the deformation modes is developed and exemplified using *piezoelectric actuators*. The PCID solution is

used to construct a set of algebraic equations that are solved for the PZT voltages. The implementation of the proposed actuation and control approach is demonstrated using a planar two-link flexible-robot manipulator. The results obtained in this investigation demonstrate deterioration in the robot performance by relying only on the joint actuation and not considering the deformation actuation.

In this study, it is assumed that the motion trajectories are specified at the position level using holonomic constraint equations. The case of nonholonomic constraints which cannot be integrated to obtain constraints between coordinates is not considered in this investigation. For nonholonomic systems, the number of independent coordinates is different from the number of independent velocities. That is, nonholonomic constraints do not impose restrictions on the coordinates. This is an important problem since the actuation is associated with the number of degrees of freedom of the system that must be controlled. One can use an inverse-dynamics procedure similar to the one used in this investigation in the case of linear nonholonomic constraint equations. Lagrange multipliers associated with the nonholonomic constraints can be used to determine the actuation forces that ensure that the nonholonomic constraints are imposed on the velocities. However, the variations in the coordinates are not governed by these nonholonomic constraint equations. A more detailed and thorough analysis is required to be able to address this problem and have a good understanding of the control of flexible-robot systems subjected to nonholonomic velocity constraints.

Acknowledgment

This research was supported, in part, by the National Science Foundation (Projects # 1852510).

Conflict of Interest

There are no conflicts of interest.

Data Availability Statement

The data sets generated and supporting the findings of this article are obtainable from the corresponding author upon reasonable request. The authors attest that all data for this study are included in the paper. Data provided by a third party are listed in Acknowledgment.

References

[1] Book, W. J., 1981, "Recursive Lagrangian Dynamics of Flexile Manipulator Arms," Int. J. Rob. Res., **3**(3), pp. 87–101.
[2] Dwivedy, S. K., and Eberhard, P., 2006, "Dynamic Analysis of Flexible Manipulators, A Literature Review," Mech. Mach. Theory, **41**(7), pp. 749–777.
[3] Rahimi, H. N., and Nazemizadeh, M., 2014, "Dynamic Analysis and Intelligent Control Techniques for Flexible Manipulators: A Review," Adv. Rob., **28**(2), pp. 63–76.
[4] Kiang, C. T., Spowage, A., and Yoong, C. K., 2015, "Review of Control and Sensor System of Flexible Manipulator," J. Intell. Rob. Syst., **77**(1), pp. 187–213.
[5] Sayahkarajy, M., Mohamed, Z., and Faudzi, A. A. M., 2016, "Review of Modelling and Control of Flexible-Link Manipulators," Proc. Inst. Mech. Eng. Part I J. Syst. Control Eng., **230**(8), pp. 861–873.
[6] Subedi, D., Tyapin, I., and Hovland, G., 2020, "Review on Modeling and Control of Flexible Link Manipulators," Model. Ident. Control, **41**(3), pp. 141–163.
[7] Kraus, K., Sika, Z., Benes, P., Krivosei, J., and Vyhlidal, T., 2020, "Mechatronic Robot Arm With Active Vibration Absorbers," J. Vib. Control, **26**(13–14), pp. 1145–1156.
[8] Wang, P., Zhang, D., and Lu, B., 2020, "Trajectory Tracking Control for Chain-Series Robot Manipulator: Robust Adaptive Fuzzy Terminal Sliding Mode Control With Low-Pass Filter," Int. J. Adv. Rob. Syst., **17**(3), pp. 1–12.
[9] Liang, L., Le, Z., Zhang, S., and Li, J., 2020, "Modeling and Controller Design of an Active Motion Compensated Gangway Based on Inverse Dynamics in Joint Space," Ocean Eng., **197**, p. 106864.
[10] Pereira, E., Ciudad, R., Aphale, S. S., Feliu, V., and Moheimani, S. O. R., 2009, "A Hybrid Control Strategy for Vibration Damping and Precise Tip-Positioning of a Single-Link Flexible Manipulator," ICM2009 IEEE International Conference on Mechatronics, Malaga, Spain, April, pp. 1–6.
[11] Pereira, E., Trapero, J. R., Dıaz, I. M., and Feliu, V., 2009, "Adaptive Input Shaping for Maneuvering Flexible Structures Using an Algebraic Identification Technique," Automatica, **45**(4), pp. 1046–1051.
[12] Sabatini, M., Gasbarri, P., Monti, R., and Palmerini, G. B., 2012, "Vibration Control of a Flexible Space Manipulator During on Orbit Operations," Acta Astronaut., **73**, pp. 109–121.
[13] Suarez, A., Giordano, A. M., Kondak, K., Heredia, G., and Ollero, A., 2018, "Flexible Link Long Reach Manipulator With Lightweight Dual Arm: Soft-Collision Detection, Reaction, and Obstacle Localization," 2018 IEEE International Conference on Soft Robotics (RoboSoft), Livorno, Italy, Apr. 24–28, pp. 406–411.
[14] Qiu, Z. C., and Zhang, W. Z., 2019, "Trajectory Planning and Diagonal Recurrent Neural Network Vibration Control of a Flexible Manipulator Using Structural Light Sensor," Mech. Syst. Signal Process., **132**, pp. 563–594.
[15] Comi, F., Miguel, A. O., Cavenago, F., Ferretti, G., Magnani, G., and Rusconi, A., 2019, "Modelling, Validation and Control of DELIAN Flexible Manipulator," IFAC-PapersOnLine, **52**(15), pp. 364–369.
[16] Runciman, M., Darzi, A., and Mylonas, G. P., 2019, "Soft Robotics in Minimally Invasive Surgery," Soft Rob., **6**(4), pp. 423–443.
[17] Lei, R. H., and Chen, L., 2020, "Finite-Time Tracking Control and Vibration Suppression Based on the Concept of Virtual Control Force for Flexible Two-Link Space Robot," Def. Technol., **17**, pp. 874–883.
[18] Matsuno, F., and Yamamoto, K., 1993, "Dynamic Hybrid Position/Force Control of a Flexible Manipulator," Proceedings of 1993 IEEE International Conference on Robotics and Automation, Atlanta, GA, May 2–6, pp. 462–467.
[19] Lochan, K., Roy, B. K., and Subudhi, B., 2016, "A Review on Two-Link Flexible Manipulators," Ann. Rev. Control, **42**, pp. 346–367.
[20] Lochan, K., and Roy, B. K., 2018, "Second-Order SMC for Tip Trajectory Tracking and Tip Deflection Suppression of an AMM Modelled Nonlinear TLFM," Int. J. Dyn. Control, **6**(3), pp. 1310–1318.
[21] Singh, N., and Rajendran, S., 2016, "Integral Fast Output Sampling Control for Flexible Link Manipulators With LMI Approach," Proceeding of the IEEE 1st International Conference on Power Electronics, Intelligent Control and Energy Systems, Delhi, India, July 4–6, pp. 1–6.
[22] Reddy, M. P. P., and Jacob, J., 2017, "Vibration Control of Flexible Link Manipulator Using SDRE Controller and Kalman Filtering," Stud. Inform. Control, **26**(2), pp. 143–150.
[23] Bazaei, A., and Moallem, M., 2010, "Improving Force Control Bandwidth of Flexible-Link Arms Through Output Redefinition," IEEE/ASME Trans. Mechatron., **16**(2), pp. 380–386.
[24] Pradhan, S. K., and Subudhi, B., 2020, "Position Control of a Flexible Manipulator Using a New Nonlinear Self-tuning PID Controller," IEEE/CAA J. Autom. Sin., **7**(1), pp. 136–149.
[25] Vijay, M., and Jena, D., 2018, "Backstepping Terminal Sliding Mode Control of Robot Manipulator Using Radial Basis Functional Neural Networks," Comput. Electr. Eng., **67**, pp. 690–707.
[26] Liu, H., and Zhang, T., 2012, "Fuzzy Sliding Mode Control of Robotic Manipulators With Kinematic and Dynamic Uncertainties," J. Dyn. Syst., Meas., Control, **134**(6), pp. 72–80.
[27] Ahmad, M. A., Tumari, M. Z. M., and Nasir, A. N. K., 2013, "Composite Fuzzy Logic Control Approach to a Flexible Joint Manipulator," Int. J. Adv. Rob. Syst., **10**(1), pp. 58–66.
[28] Ho, H. F., Wong, Y. K., and Rad, A. B., 2007, "Robust Fuzzy Tracking Control for Robotic Manipulators," Simul. Modell. Pract. Theory, **15**(7), pp. 801–816.
[29] Sarkhel, P., Banerjee, N., and Hui, N. B., 2020, "Fuzzy Logic-Based Tuning of PID Controller to Control Flexible Manipulators," SN Appl. Sci., **2**(6), pp. 1124–1134.
[30] Zhang, L., and Liu, J., 2013, "Adaptive Boundary Control for Flexible Two-Link Manipulator Based on Partial Differential Equation Dynamic Model," IET Control Theory Appl., **7**(1), pp. 43–51.
[31] Macnab, C. J. B., 2009, "Stable Neural Control of a Flexible-Joint Manipulator Subjected to Sinusoidal Disturbance," Proceedings of the Fourth International Conference on Autonomous Robots and Agents, Wellington, New Zealand, Feb. 10–12, pp. 698–703.
[32] Neto, A. D., Goes, L. C. S., and Nascimento, C. L., 2010, "Accumulative Learning Using Multiple ANN for Flexible Link," IEEE Trans. Aerosp. Electr. Syst., **46**(2), pp. 508–524.
[33] Kozel, D., Koivo, A. J., and Mahil, S. S., 1991, "General Force/Torque Relationship and Kinematic Representation for Flexible Link Manipulators," J. Rob. Syst., **8**(4), pp. 531–556.
[34] Gofron, M., and Shabana, A. A., 1993, "Control Structure Interaction in the Nonlinear Analysis of Flexible Mechanical Systems," Nonlinear Dyn., **4**, pp. 183–206.
[35] Gofron, M., and Shabana, A. A., 1995, "Equivalence of the Driving Elastic Forces in Flexible Multibody System," Int. J. Numer. Methods Eng., **38**(17), pp. 2907–2928.
[36] Lee, B. H., 2003, "Inverse Dynamic Analysis of Mechanical Systems in Joint Coordinate Space," Proc. Inst. Mech. Eng. Part K J. Multi-body Dyn., **217**(1), pp. 29–37.
[37] Ata, A. A., 2010, "Inverse Dynamic Analysis and Trajectory Planning for Flexible Manipulator," Inverse Prob. Sci. Eng., **18**(4), pp. 549–566.
[38] Yang, K., Yang, W., and Wang, C., 2018, "Inverse Dynamic Analysis and Position Error Evaluation of the Heavy-Duty Industrial Robot With Elastic Joints: An Efficient Approach Based on Lie Group," Nonlinear Dyn., **93**(2), pp. 487–504.
[39] Lauß, T., Oberpeilsteiner, S., Sherif, K., and Steiner, W., 2019, "Inverse Dynamics of an Industrial Robot Using Motion Constraints," Proceeding of the

20th International Conference on Research and Education in Mechatronics (REM), Wels, Austria, May 23–24, pp. 1–7.
[40] Lismonde, A., Sonneville, V., and Brüls, O., 2019, "A Geometric Optimization Method for the Trajectory Planning of flexible Manipulators," Multibody Sys. Dyn., **47**(4), pp. 347–362.
[41] Rong, Y., Zhang, X. C., and Qu, M. K., 2019, "Unified Inverse Dynamics for a Novel Class of Metamorphic Parallel Mechanisms," Appl. Math. Model., **74**, pp. 280–300.
[42] Ren, H., and Ben-Tzvi, P., 2020, "Learning Inverse Kinematics and Dynamics of a Robotic Manipulator Using Generative Adversarial Networks," Rob. Auton. Syst., **124**, p. 103386.
[43] Bansevicius, R., and Tolocka, R. T., 2002, "Piezoelectric Actuators," *Mechatronics Handbook*, CRC Press, Boca Raton, FL.
[44] Ouyang, P. R., Tjiptoprodjo, R. C., Zhang, W. J., and Yang, G. S., 2008, "Micro-motion Devices Technology: The State of Arts Review," Int. J. Adv. Manuf. Technol., **38**(5–6), pp. 463–478.
[45] Zheng, L., Chen, W., and Huo, D., 2020, "Review of the Vibration Devices for Vibration-Assisted Machining," Int. J. Adv. Manuf. Technol., **108**(5–6), pp. 1631–1651.
[46] Choi, S. B., Cho, S. S., Shin, H. C., and Kim, H. K., 1999, "Quantitative Feedback Theory Control of a Single-Link Flexible Manipulator Featuring Piezoelectric Actuator and Sensor," Smart Mater. Struct., **8**(3), pp. 338–349.
[47] Shin, H. C., and Choi, S. B., 2001, "Position Control of a Two-Link Flexible Manipulator Featuring Piezoelectric Actuators and Sensors," Mechatronics, **11**(6), pp. 707–729.
[48] Sun, D., Shan, J., Su, Y., Liu, H. H. T., and Lam, C., 2005, "Hybrid Control of a Rotational Flexible Beam Using Enhanced PD Feedback With a Nonlinear Differentiator and PZT Actuators," Smart Mater. Struct., **14**(1), pp. 69–78.
[49] Bottega, V., Molter, A., Fonseca, J. S. O., and Pergher, R., 2009, "Vibration Control of Manipulators With Flexible Nonprismatic Links Using Piezoelectric Actuators and Sensors," Math. Probl. Eng., **2009**, Article ID 727385, pp. 1–16.
[50] Jain, R. K., Majumder, S., Ghosh, B., and Saha, S., 2015, "Deflection Control for Piezoelectric Actuator Through Voltage Signal and Its Application in Micromanipulation," Mech. Syst. Signal Process, **62–63**, pp. 305–323.
[51] Gurses, K., Buckham, B. J., and Park, E. J., 2009, "Vibration Control of a Single-Link Flexible Manipulator Using an Array Of Fiber Optic Curvature Sensors and PZT Actuators," Mechatronics, **19**(2), pp. 167–177.
[52] Lou, J., Wei, Y., Li, G., Yang, Y., and Xie, F., 2015, "Optimal Trajectory Planning and Linear Velocity Feedback Control of a Flexible Piezoelectric Manipulator for Vibration Suppression," Shock Vib., **2015**, Article ID 952708, pp. 1–11.
[53] Zhang, Q., Li, C., Zhang, J., and Zhang, J., 2017, "Smooth Adaptive Sliding Mode Vibration Control of a Flexible Parallel Manipulator With Multiple Smart Linkages in Modal Space," J. Sound Vib., **411**, pp. 1–19.
[54] Chen, T., Wang, Y., Yang, Z., Liu, H., Liu, J., and Sun, L., 2017, "A PZT Actuated Triple-Finger Gripper for Multi-Target Micromanipulation," Micromachines, **33**(8), pp. 1–11.
[55] Shao, M., Huang, Y., and Silberschmidt, V. V., 2020, "Intelligent Manipulator With Flexible Link and Joint: Modeling and Vibration Control," Shock Vib., **2020**, Article ID 4671358, pp. 1–15.
[56] Ma, K., and Ghasemi-Nejhad, M. N., 2008, "Adaptive Control of Flexible Active Composite Manipulators Driven by Piezoelectric Patches and Active Struts With Dead Zones," IEEE Trans. Control Syst. Technol., **16**(5), pp. 897–907.
[57] Dong, X. J., Meng, G., and Peng, J. C., 2006, "Vibration Control of Piezoelectric Smart Structures Based on System Identification Technique: Numerical Simulation and Experimental Study," J. Sound Vib., **297**(3–5), pp. 680–693.
[58] Sun, D., Mills, J. K., Shan, J., and Tso, S. K., 2004, "A PZT Actuator Control of A Single-Link Flexible Manipulator Based on Linear Velocity Feedback and Actuator Placement," Mechatronics, **14**(4), pp. 381–401.
[59] Zhang, X., Mills, J. K., and Cleghorn, W. L., 2008, "Vibration Control of Elastodynamic Response of a 3-PRR Flexible Parallel Manipulator Using PZT Transducers," Robotica, **26**(5), pp. 655–665.
[60] Asada, H., Ma, Z. D., and Tokumaru, H., 1990, "Inverse Dynamics of Flexible Robot Arms: Modeling and Computation for Trajectory Control," AMSE J. Dyn. Syst. Meas. Contr., **112**(2), pp. 177–185.
[61] Bayo, E., Papadopoulos, P., Stubbe, J., and Serna, M. A., 1989, "Inverse Dynamics and Kinematics of Multi-link Elastic Robots: An Iterative Frequency Domain Approach," Int. J. Rob. Res., **8**(6), pp. 49–62.
[62] Carrera, E., and Serna, M. A., 1996, "Inverse Dynamics of Flexible Robots," Math. Comput. Simul., **41**(5–6), pp. 485–508.
[63] Beres, W., Sasiadek, J. Z., and Vukovich, G., 1993, "Control and Dynamic Analysis of Multilink Flexible Manipulator," Proceedings—IEEE International Conference on Robotics and Automation, Vol. 3, pp. 478–483.
[64] Theodore, R. J., and Ghosal, A., 1995, "Comparison of the Assumed Modes and Finite Element Models for Flexible Multilink Manipulators," Int. J. Rob. Res., **14**(2), pp. 91–111.
[65] Kim, J. S., and Uchiyama, M., 2003, "Vibration Mechanism of Constrained Spatial Flexible Manipulators," JSME Int. J., Ser. C, **46**(1), pp. 123–128.
[66] Fotouhi, R., 2007, "Dynamic Analysis of Very Flexible Beams," J. Sound Vib., **305**(3), pp. 521–533.
[67] Celentano, L., and Coppola, A. A., 2011, "Computationally Efficient Method for Modeling Flexible Robots Based on the Assumed Modes Method," Appl. Math. Comput., **218**(8), pp. 4483–4493.
[68] Korayem, M. H., Rahimi, H. N., and Nikoobin, A., 2012, "Mathematical Modeling and Trajectory Planning of Mobile Manipulators With Flexible Links And Joints," Appl. Math. Model., **36**(7), pp. 3229–3244.
[69] Vakil, M., Fotouhi, R., and Nikiforuk, P. N., 2012, "A New Method for Dynamic Modeling Of Flexible-Link Flexible-Joint Manipulators," ASME J. Vib. Acoust., **134**(1), p. 014503.
[70] Shabana, A. A., 2020, *Dynamics of Multibody Systems*, 5th ed., Cambridge University Press, Cambridge, UK.
[71] Zhang, Q., Mills, J. K., Cleghorn, W. L., Jin, J., and Zhao, C., 2015, "Trajectory Tracking and Vibration Suppression of a 3-PRR Parallel Manipulator With Flexible Links," Multibody Sys. Dyn., **33**(1), pp. 27–60.
[72] Kang, B., and Mills, J. K., 2005, "Vibration Control of a Planar Parallel Manipulator Using Piezoelectric Actuators," J. Intell. Rob. Syst., **42**(1), pp. 51–70.
[73] Gilardi, G., Buckham, B. J., and Park, E. J., 2009, "Finite Element Modeling of a Slewing Non-linear Flexible Beam for Active Vibration Control With Arrays of Sensors and Actuators," J. Intell. Mater. Syst. Struct., **20**(16), pp. 1941–1958.
[74] Lu, E., Li, W., Yang, X., Fan, M., and Liu, Y., 2016, "Modelling and Composite Control of Single Flexible Manipulators With Piezoelectric Actuators," Shock Vib., **2016**, Article ID 2689178, pp. 1–14.
[75] Wei, J. J., Qiu, Z. C., Han, J. D., and Wang, Y. C., 2010, "Experimental Comparison Research on Active Vibration Control for Flexible Piezoelectric Manipulator Using Fuzzy Controller," J. Intell. Rob. Syst., **59**(1), pp. 31–56.
[76] Yan, A. Z., Wang, G. Q., Xu, H., and Sheng, Y., 2004, "Reduction of Residual Vibration in a Rotating Flexible Beam," Acta Mech., **171**(3–4), pp. 137–149.
[77] Maxwell, N. D., and Asokanthan, S. F., 2003, "Optimally Distributed Actuator Placement and Control for a Slewing Single-Link Flexible Manipulator," Smart Mater. Struct., **12**(2), pp. 287–296.
[78] Yan, X. J., and Yam, L. H., 2002, "Optimal Design of Number and Locations of Actuators in Active Vibration Control of a Space Truss," Smart Mater. Struct., **11**(4), pp. 496–593.
[79] Shabana, A. A., Eldeeb, A. E., and Bai, Z., 2021, "Near-Elimination of Small Oscillations of Articulated Flexible-Robot Systems," Sound Vib., **500**, p. 116015.